ELSEVIER

Journal of Pharmaceutical and Biomedical Analysis
29 (2002) 307–315

JOURNAL OF
PHARMACEUTICAL
AND BIOMEDICAL
ANALYSIS

www.elsevier.com/locate/jpba

# Some kinetic aspects in the immunoradiometric assay of insulin-like growth factor binding protein-3

J. García Gómez, M. Porcar Pons, J.L. Moreno Frigols *

*Department of Physical Chemistry*, *Faculty of Pharmacy*, *Radioisotope Service*, *Valencia University Hospital*, *Valencia*, *Spain*

Received 6 October 2001; received in revised form 28 January 2002; accepted 16 February 2002

**Abstract**

In this article the kinetics of the insulin-like growth factor binding protein-3 (IGFBP-3) reaction with its specific antibody immobilised on the inner wall of the reaction tube, and the subsequent binding of the immunocomplex formed with a second $^{125}$I-labelled antibody are described. These reactions are used in the immunoradiometric determination of IGFBP-3. Independent variables were analyte and labelled antibody, temperature, viscosity, and the ionic strength of the medium. For the global process mono-exponential kinetics were found to be dependent on the concentrations, such dependence fitting with the models discussed in this paper. Viscosity results clearly indicate its negative influence on the direct reaction rate. Ionic strength shows noticeable but not too relevant effects, which suggests that the variation caused by the glycerol addition is not due to the influence of the dielectric constant of the solutions used. The effect of temperature shows activation parameters similar to the viscous flow energy of water, which suggests diffusion control for the global process. 

*Keywords:* Kinetics; Immunoradiometric assay; Insulin-like growth factor binding protein-3; Viscosity; Ionic strength; Temperature; Diffusion

## 1. Introduction

The determination of insulin-like growth factor binding protein-3 (IGFBP-3) serum levels has been proposed as the best indicator of growth hormone deficiency (GHD) during the first 5 years of life because of the poor discrimination value of IGF-1 levels. In patients with GHD, the response of IGFBP-3 to GH administration is low (maximum after 4 days). In contrast, the response of IGF-1 administration is considerably faster (maximum after 4 h) indicating that IGFBP-3 may be regulated by IGF-1 rather than GH.

Immunoradiometric assay (IRMA) is used in IGFBP-3 assessment. It is based on the determination of an analyte by using a labelled antibody [1]. This technique may be competitive or not, but in this particular case the non-competitive model has been chosen. Thus the sample or calibrated solution is incubated in a test tube whose inner wall is antibody-coated. Next, a second-labelled

* Corresponding author. Address: Dpto. Química Física, Facultad de Farmacia, Avda. Vicent Andrés Estellés s/n, 46110 Burjassot, Valencia, Spain. Tel.: +34-96-3864894; fax: +34-96-3864892.

*E-mail address:* jose.l.moreno@uv.es (J.L. Moreno Frigols).

0731-7085/02/$ - see front matter 
PII: S0731-7085(02)00090-0

antibody is added, thus making a 'sandwich' in which the radioactivity retained increases with the presence of the antigen in the sample. This antibody is aimed at a second antigenic determinant of the antigen molecule i.e. the antigen will bind to both antibodies through different molecules areas.

Kinetics and equilibrium in antigen–antibody reactions are determining factors in the sensitiveness and accuracy of the immunoanalytical techniques. In previous research [2,3], different characteristics have been studied in relation with the antigen–antibody reactions used in analytical techniques, that employ radioactivity as a measurable magnitude. The results suggest diffusive control in this type of processes. Stenberg et al. [4–7] proposed an application model for reactions occurring in the solid–liquid interphase and provided an equation with four parameters that indicated diffusion influence.

Equilibrium data analysis is used to a great extent in determining the capacity of a substance to bind to one or several receptor populations. Nonetheless, as pointed out by Weber [8], detecting two binding sites through such an assay requires the ligand to have very different affinity for the two binding sites.

Motulsky and Mahan [9] and later on Karlsson and Neil [10] noticed that the distinction between single-site binding and two-site binding models was in many cases impossible through equilibrium analysis, while at the same time it was indeed feasible on the basis of kinetic experiments. The latter authors proposed a method which was applied to the study of the binding of titriade Noscapine (antitussive) to guinea pig brain homogenate which can have a general application for single- and double-site binding model receptor populations with ligand excess. This would allow for the discrimination between binding models and the study of binding parameters by using kinetic data only.

Xavier and Willson [11,12] studied the association and dissociation reactions of hen egg lysozime (HEL) with two of its specific antibodies (HyHEL-5 and HyHEL-10) under pseudo first-order conditions for the association, and found diffusion control. The decrease in the reaction rate constants as a result of viscosity turned out to be more drastic than theoretically expected, this aspect being put down to potential osmotic effects. In addition, rate constants were found to approximately double when ionic strength goes down from 500 to 27 mM, which indicates that the process occurs between species with opposite charges that affect the orientational requirements of association.

A diffusion-controlled process should meet some standard requirements such as a considerable reaction rate decrease when medium viscosity is greater, and slight temperature influence with a reduced energy demand with regards activation, this causing activation enthalpy values to be of the same order as the solvent's viscous flow energy (5000 cal/mol for water).

This article focuses on the kinetics of the reactions between IGFBP-3 and its specific antibodies, and studies the influence of the concentration of the reagents for both the global reaction and its stages, as well as the effect of temperature. As a complementary factor, the influence of viscosity on such processes is analysed. The media have different dielectric constants which—should the reaction occur between charged species—would give way to an effect that would overlap with that of viscosity. In order to indirectly estimate this potential influence, reactions are studied in media with different ionic strength.

Our target is to characterise immunoradiometric reactions and in particular those used in IGFBP-3 measurement, based on the following steps:

1. Obtaining integrated rate equations for the overall process.
2. Rate comparison for the different process stages in order to establish the potential reaction mechanism.
3. Setting up the possible diffusion control through the study of viscosity and temperature influence upon reaction kinetics.
4. Complementary study of ionic strength with a view to either including or ruling out the effect of the electrical charges.

## 2. Material and methods

### 2.1. Reagents

1. Solution of $^{125}$I-labelled monoclonal anti-IGFBP-3 mouse antibodies.
2. Tubes coated with monoclonal antibodies antiIGFBP-3.
3. IGFBP-3 standard solutions.

All the reagents used were included in the IGFBP-3 IRMA kit manufactured by Immunotech.

### 2.2. Instruments

LKB Gammamaster Automatic Gamma Counter. Brookfield DV-II digital viscosimeter. Viscosity measurements were performed at 60 rpm with a UL ADADPTER at 26.5 °C.

### 2.3. Experimental procedure

Reaction kinetics were studied by placing the reagents in the coated tubes and letting them react at different times. Once the reaction time elapsed, radioactivity was measured for each tube by the gamma counter.

| | | | | | | | | | | | | | | | | |
|---|---|---|---|---|---|---|---|---|---|---|---|---|---|---|---|---|
| Tracer | 0.2 | 0.4 | 0.7 | 1.0 | 0.2 | 0.4 | 0.7 | 1.0 | 0.2 | 0.4 | 0.7 | 1.0 | 0.2 | 0.4 | 0.7 | 1.0 |
| Glycerol | 0.0 | 0.0 | 0.0 | 0.0 | 0.2 | 0.2 | 0.2 | 0.2 | 0.4 | 0.4 | 0.4 | 0.4 | 0.6 | 0.6 | 0.6 | 0.6 |
| Distilled $H_2O$ | 2.6 | 2.4 | 2.1 | 1.8 | 2.4 | 2.2 | 1.9 | 1.6 | 2.2 | 2.0 | 1.7 | 1.4 | 2.0 | 1.8 | 1.5 | 1.2 |
| $\eta$ (mPa s) | 1.368 | | | | 1.458 | | | | 1.577 | | | | 1.745 | | | |

Fifty-nine experiments were performed, arranged as follows:

#### 2.3.1. Experiments 1–9

Study of the influence of tiroglobuline (Q) and tracer (M) concentrations upon the global reaction. Fifty microlitre of Q and 200 μl of M from different concentrations were left to react.

#### 2.3.2. Experiments 10–12

Study of the influence of the concentrations of the previously mentioned factors upon the first process stage i.e. upon the binding of Q to the antibody bound to the tube wall (P). Q-coated tubes were incubated at different times; later on and once washed, M was added and it was left to react for 24 h.

#### 2.3.3. Experiments 13–15

Study of the influence of the same factors upon the second process stage, namely the biding of M to the PQ immunocomplex. Tubes and Q were left to react for 24 h, and once washed M was added and it was left to react at different times.

#### 2.3.4. Experiments 16–27

Study of the influence of temperature. Four experiments were carried out at constant Q and at four different temperatures.

#### 2.3.5. Experiments 28–43

Study of the influence of viscosity at Q and M constant concentrations using four solutions prepared as per the table below (quantities in ml). In the experiments, 200 μl of the solutions were taken and left to react with 50 μl of Q. Final viscosity of the solutions obtained in this manner was determined by comparison with a calibration curve drawn from standard glycerol–water mixes.

#### 2.3.6. Experiments 44–59

Study of the influence of ionic strength at Q and M constant concentrations, using four solutions prepared as per the table below (quantities in ml). In the experiments, 200 μl of the solutions were taken and left to react with 50 μl of Q. Final ionic strength of the reacting mixes obtained in this manner are shown in the table.

| | | | | | | | | | | | | | | | | |
|---|---|---|---|---|---|---|---|---|---|---|---|---|---|---|---|---|
| Tracer | 0.2 | 0.4 | 0.7 | 1.0 | 0.2 | 0.4 | 0.7 | 1.0 | 0.2 | 0.4 | 0.7 | 1.0 | 0.2 | 0.4 | 0.7 | 1.0 |
| CINa 0.410 M | 0.2 | 0.2 | 0.2 | 0.2 | 0.4 | 0.4 | 0.4 | 0.4 | 0.6 | 0.6 | 0.6 | 0.6 | 0.8 | 0.8 | 0.8 | 0.8 |
| Distilled $H_2O$ | 2.4 | 2.2 | 1.9 | 1.6 | 2.2 | 2.0 | 1.7 | 1.4 | 2.0 | 1.8 | 1.5 | 1.2 | 1.8 | 1.6 | 1.5 | 1.2 |
| $I$ (mol/l) | 0.023 | | | | 0.047 | | | | 0.070 | | | | 0.094 | | | |

### 2.4. Data analysis

The statistical programme was used with specific non-linear regression equations. As the statistical criterion that allows a choice from different equations, AIC was observed (Akaike's Information Criterion), expressed as $AIC = N\ln S + 2P$ where $N$ is the number of points, $S$ the addition of residual squares, and $P$ the number of parameters in the equation. The fitting with the lowest AIC must be chosen.

### 2.5. Symbols

| | |
|---|---|
| P | antibody bound to the tube wall |
| Q | IGFBP-3 |
| M | $^{125}$I-labelled antiIGFBP-3 antibody |
| PQ | immunocomplex made of the antibody bound to the tube with the IGFBP-3 |
| PQM | sandwich-type radioactive immunocomplex |
| [P], [Q], [M], [PQ], [PM] | mol/l concentrations |
| $P_0$, $M_0$, $Q_0$ | initial concentrations in arbitrary units |
| $Z$ | cpm activity measured in each tube after reaction ($Z = Z_{sp} + Z_0$). A sub-index is added in the tables indicating the experiment number |
| $Z_{sp}$ | activity specifically bound to the tube wall, directly proportional to the radioactive immunocomplex concentration |
| $Z_0$ | value of $Z$ obtained at $t = 0$. Corresponds to unspecific binding |
| $Z_\infty$ | value of $Z$ obtained at $t$ infinity |
| $Z_e$ | value of $Z_{sp}$ at equilibrium ($Z_e = Z_\infty - Z_0$) |
| $t$ | time, in min |
| $T$ | temperature, K |
| $v_0$ | initial rate |
| $k$ | rate constant |
| $K$ | equilibrium constant |
| $\eta$ | viscosity (mPa s) |
| $I$ | ionic strength (mol/l) |
| $z$ | charge of chemical species |
| $r$ | correlation coefficient |
| $s$ | addition of residual squares |

## 3. Results and discussion

### 3.1. Influence of M and Q concentrations. Global reaction (Experiments 1–9, Table 1, Fig. 1a) and stages (Experiments 10–15, Table 2)

This is the global process:

$$P + Q + M \rightarrow PQM$$

It can be broken down as follows:

$$P + Q \underset{k_{-1}}{\overset{k_1}{\Leftrightarrow}} PQ \text{ (quick)} \quad \text{and}$$
$$PQ + M \underset{k_{-2}}{\overset{k_2}{\Leftrightarrow}} PQM \text{ (slow)}$$

The second stage is slower, as can be seen in Table 2, the initial velocities of this stage are rather close to the global process's at equal concentrations (Table 1). If it is assumed that quick equilibrium is reached, then:

$$\frac{[PQ]}{[P_0][Q]} = \frac{k'_1}{k_{-1}} \qquad [PQ] = \frac{[P_0][Q]}{[Q] + \frac{k_{-1}}{k'_1}}$$

Table 1
Influence of M and Q concentrations (global reaction)

| $t$ (min) | 0 | 15 | 60 | 120 | 180 | 300 | ∞ | $v_0$ | M | Q |
|---|---|---|---|---|---|---|---|---|---|---|
| $Z_1$ | 319.5 | 1838.0 | 7982.7 | 13285.5 | 17004.4 | 26839.5 | 36643.1 | 161.9 ($r = 1.000$) | 100 | 50 |
| $Z_2$ | 186.7 | 1517.8 | 7015.8 | 12315.0 | 15236.0 | 20322.6 | 32126.9 | 142.8 ($r = 0.999$) | 80 | 50 |
| $Z_3$ | 806.6 | 1392.3 | 5325.9 | 8676.4 | 12339.9 | 16057.6 | 24508.5 | 82.7 ($r = 0.999$) | 60 | 50 |
| $Z_4$ | 206.0 | 1115.1 | 3935.2 | 6494.9 | 8037.7 | 10443.8 | 16787.4 | 76.7 ($r = 1.000$) | 40 | 50 |
| $Z_5$ | 191.1 | 599.3 | 2274.5 | 3647.5 | 4477.3 | 5645.8 | 8721.9 | 43.1 ($r = 0.999$) | 20 | 50 |
| $Z_6$ | 342.7 | 340.9 | 1079.9 | 1703.3 | 2080.2 | 3557.8 | 7619.8 | 18.3 ($r = 0.996$) | 100 | 2.0 |
| $Z_7$ | 329.7 | 508.5 | 1672.6 | 2518.7 | 2714.9 | 6764.5 | 15016.6 | 38.6 ($r = 0.998$) | 100 | 3.33 |
| $Z_8$ | 188.0 | 788.0 | 3423.0 | 5474.0 | 6618.3 | 8271.1 | 33482.1 | 68.4 ($r = 0.999$) | 100 | 10.0 |
| $Z_9$ | 141.1 | 1617.3 | 7623.4 | 12674.7 | 15729.5 | 18046.0 | 33482.1 | 150.1 ($r = 1.000$) | 100 | 33.3 |

Globally, the values fit with the equation: $Z = \frac{a\mathrm{M}_0\mathrm{Q}_0}{(\mathrm{M}_0+b)(\mathrm{Q}_0+c)}(1-\exp(-(d(\mathrm{M}_0+e\mathrm{Q}_0+f))t))+g$. This is identical to Eq. (7). Its parameters and coefficient are: $a = 189100$, $b = 361$, $c = 6.49$, $d = 6.27\times10^{-6}$, $e = 8.84$, $f = 73.3$, $g = 421$, $r = 0.996$, $s = 43.5\times10^{6}$.

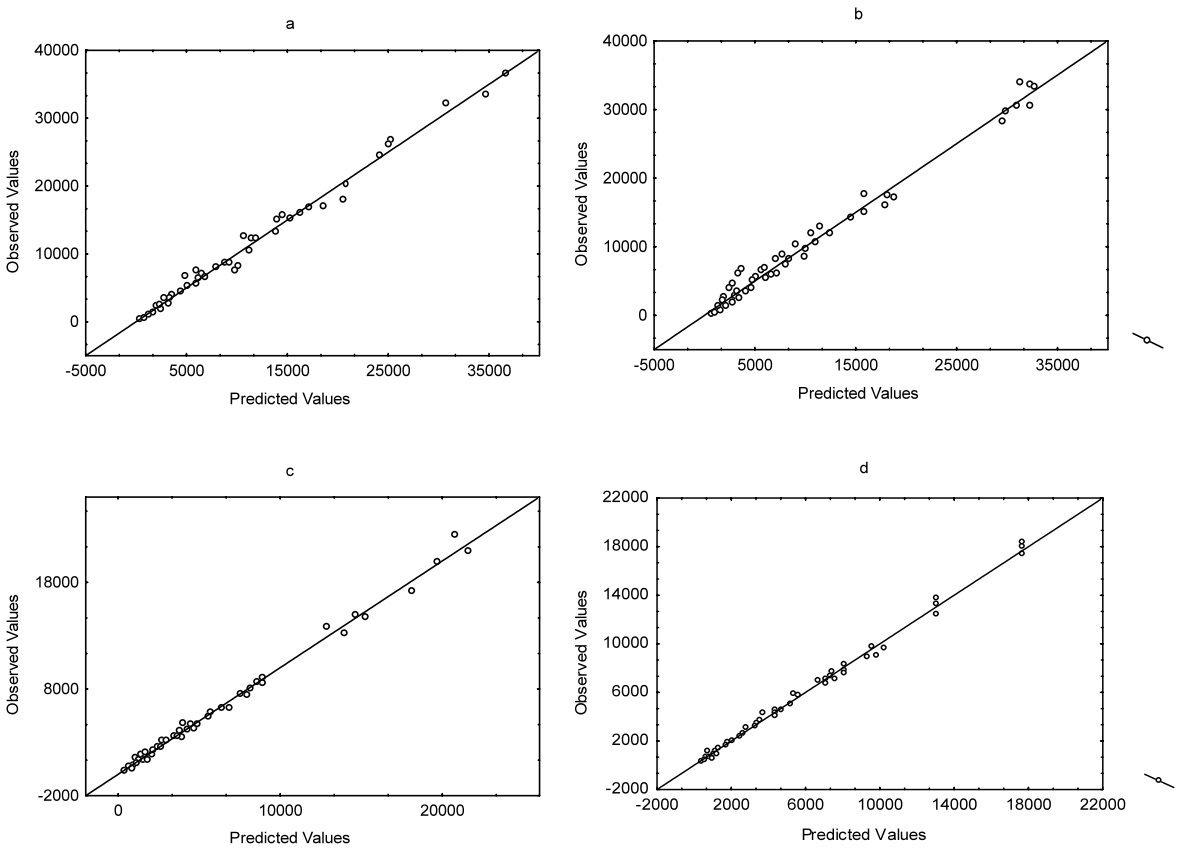


Fig. 1. (a) $Z$ values observed in Experiments 1–9 (Table 1) vs. values predicted for Eq. (7). Observed values = 0.00009 + 1.000 × Predicted values, $r = 0.996$, (b) Z values observed in Experiments 16–27 (Table 3) vs. values predicted for Eq. (8). Observed values = 0.00001 + 1.000 × Predicted values, $r = 0.993$, (c) Z values observed in Experiments 28–43 (Table 4) vs. values predicted for Eq. (9). Observed values = −0.1803 + 1.000 × Predicted values, $r = 0.996$, (d) Z values observed in Experiments 44–59 (Table 5) vs. values predicted for Eq. (10). Observed values = 0.00484 + 1.000 × Predicted values, $r = 0.998$.

Table 2
Influence of M and Q concentrations (stages)

| Stage 1 | | | | | | | | | | |
|---|---|---|---|---|---|---|---|---|---|---|
| $t$ (min) | 0 | 15 | 60 | 120 | 180 | 300 | $\infty$ | $v_0$ | $M_0$ | $Q_0$ |
| $Z_{10}$ | 1102.5 | 2938.5 | 3575.8 | 4148.7 | 4244.0 | 9853.9 | 11660.8 | 64.1 ($r=0.994$) | 100 | 2.0 |
| $Z_{11}$ | 1078.2 | 8027.5 | 10959.5 | 11140.0 | 11891.5 | 12140.7 | 20851.1 | 205.4 ($r=0.934$) | 100 | 10 |
| $Z_{12}$ | 1372.9 | 17923.1 | 23250.2 | 26509.9 | 27673.7 | 29849.2 | 33942.5 | 465.0 ($r=0.943$) | 100 | 50 |
| Stage 2 | | | | | | | | | | |
| $t$ (min) | 0 | 15 | 60 | 120 | 180 | 300 | $\infty$ | $v_0$ | M | Q |
| $Z_{13}$ | 233.5 | 2792.1 | 7557.2 | 13853.1 | 17146.3 | 21614.7 | 29765.6 | 146.5 ($r=0.999$) | 100 | 50 |
| $Z_{14}$ | 230.1 | 2073.9 | 5490.5 | 9392.0 | 11902.4 | 14286.1 | 20998.4 | 92.0 ($r=1.000$) | 60 | 50 |
| $Z_{15}$ | 341.5 | 976.0 | 2194.6 | 3830.7 | 4461.8 | 5541.0 | 7695.0 | 39.5 ($r=0.999$) | 20 | 50 |

Likewise, once equilibrium is reached, the following is applicable to the second one:

$$\frac{[PQM]}{[PQ][M]}=\frac{k'_2}{k_{-2}} \qquad [PQM]=\frac{[PQ][M]}{[M]+\frac{k_{-2}}{k'_2}}$$

from which we get:

$$[PQM]=\frac{[P]_0[Q][M]}{\left([Q]+\frac{k_{-1}}{k'_1}\right)\left([M]+\frac{k_{-2}}{k'_2}\right)} \quad (1)$$

$$Z=\frac{\frac{P_0Q_0M_0}{\left(Q_0+\frac{m}{k_1}\right)\left(M_0+\frac{n}{k_2}\right)}\frac{1-\exp\{-((Q_0+M_0-2Z_e)k_2+k_{-2})t\}}{1-\frac{Z_e^2}{Q_0M_0}\exp\{-((Q_0+M_0-2Z_e)k_2+k_{-2})t\}}+Z_0}{}$$

The rate of the second stage is:

$$\frac{d[PQM]}{dt}=k'_2[PQ][M]k_{-2}[PQM] \quad (2)$$

The experimental data encompasses activities as an indirect concentration measurement. By applying suitable transformations, Eq. (1) and Eq. (2) become:

$$Z_e=\frac{P_0Q_0M_0}{\left(Q_0+\frac{m}{k_1}\right)\left(M_0+\frac{n}{k_2}\right)} \quad (3)$$

$$\frac{dZ_{sp}}{dt}=k_2(Q_0-Z_{sp})(M_0-Z_{sp})-k_{-2}Z_{sp} \quad (4)$$

The previous treatment implicitly acknowledges that $[Q]\ll[PQ]+[PQM]$

The integration of (Eq. (4)) provides the following:

$$Z=\frac{Z_e\{1-\exp(-(Q_0+M_0-2Z_e)k_2+k_{-2})t\}}{1-\left(\frac{Z_e^2}{Q_0M_0}\right)\exp\{-((Q_0+M_0-2Z_e)k_2+k_{-2})t\}}+Z_0$$

Which, taking (Eq. (3)) into account, becomes:

which can be reduced to:

$$Z=\frac{P_0Q_0M_0}{\left(Q_0+\frac{m}{k_1}\right)\left(M_0+\frac{n}{k_2}\right)}(1-\exp\{-((Q_0+M_0-2Z_e)k_2+k_{-2})t\})+Z_0 \quad (5)$$

If in Eq. (5) the approximation $Z_e=jQ_0$ is carried out (valid if $Q_0\ll P_0$), then after simplification we have:

$$Z=\frac{P_0Q_0M_0}{\left(Q_0+\frac{m}{k_1}\right)\left(M_0+\frac{n}{k_2}\right)}(1-\exp\{(-(k_2M_0+fQ_0+k_{-2}))t\})+Z_0 \quad (6)$$

Which can be written as follows:

$$Z = \frac{a\mathrm{M}_0\mathrm{Q}_0}{(\mathrm{M}_0 + b)(\mathrm{Q}_0 + c)}$$
$$(1 - \exp(-(\mathrm{d}(\mathrm{M}_0 + e\mathrm{Q}_0 + f)t))) + g \quad (7)$$

### 3.2. Influence of temperature. Experiments 16–27, Table 3, Fig. 1b

If the following is done in Eq. (7):

$$\mathrm{M}_0 \gg b, \quad c = b'\exp(-c'/T)$$

(van t'Hoff"s Equation)

$$e\mathrm{Q}_0 \gg d\mathrm{M}_0 + f \quad d = IT\exp(-e'/T)$$

(Eyring's Equation)

By putting the constants together and simplifying, then we have:

$$Z = \frac{a'\mathrm{Q}_0}{\mathrm{Q}_0 + b'\exp\left(\frac{-c'}{T}\right)}$$
$$\left\{1 - \exp\left(-\mathrm{Q}_0 d'T\exp\left(\frac{-e'}{T}\right)\right)t\right\} + f' \quad (8)$$

The activation enthalpy for the process is $\Delta H = Rm = 2 \times 2680 = 5360$ cal/mol, its magnitude order being that of the viscous flow energy of water.

### 3.3. Influence of viscosity. Experiments 28–43, Table 4, Fig. 1c

For the rate constants, standard theory on diffusion-controlled reactions [13] provides the following expression:

$$k = \frac{8RT}{3\eta}$$

Which is valid for spherical, non-ionic, and similar-radius molecules. In our case, good fitting to this equation is not found, which is not surprising at all, as not all conditions can be expected to be met. Kramers [14] pointed out that rate constants $k^0$ and $k^v$ obtained in the absence and presence of a viscosizing agent such as glycerol relate to the corresponding viscosities through the equation $\frac{k^0}{k^v} = A + B\frac{\eta}{\eta_0}$

Table 3
Influence of temperature ($\mathrm{Q}_0 = 50$)

| $t$ (min) | 0 | 15 | 60 | 120 | 180 | 300 | ∞ | $v_o$ | Qo | $T$ (K) |
|---|---|---|---|---|---|---|---|---|---|---|
| $Z_{16}$ | 188.0 | 596.5 | 1887.8 | 3769.0 | 5892.6 | 9674.3 | 30546.3 | 24.3 ($r = 1.000$) | 50 | 278 |
| $Z_{17}$ | 60.0 | 373.9 | 1409.0 | 3261.5 | 5174.5 | 8241.3 | 28326.2 | 17.3 ($r = 1.000$) | 33.3 | 278 |
| $Z_{18}$ | 242.5 | 354.1 | 597.9 | 1455.7 | 2377.5 | 4622.7 | 17736.0 | 2.9 ($r = 1.000$) | 10 | 278 |
| $Z_{19}$ | 462.5 | 675.9 | 2580.2 | 5512.7 | 8259.1 | 12028.0 | 33338.9 | 29.2 ($r = 1.000$) | 50 | 286 |
| $Z_{20}$ | 248.9 | 780.5 | 1999.5 | 4209.0 | 6860.4 | 10252.4 | 30635.5 | 18.5 ($r = 1.000$) | 33.3 | 286 |
| $Z_{21}$ | 179.6 | 158.2 | 954.3 | 2247.8 | 3669.8 | 6160.0 | 17560.5 | 8.5 ($r = 1.000$) | 10 | 286 |
| $Z_{22}$ | 142.5 | 764.0 | 3496.0 | 6098.7 | 8593.7 | 14286.6 | 33589.6 | 63.7 ($r = 1.000$) | 50 | 293 |
| $Z_{23}$ | 44.5 | 538.9 | 2882.5 | 5608.5 | 8193.0 | 12020.2 | 30506.3 | 47.2 ($r = 1.000$) | 33.3 | 293 |
| $Z_{24}$ | 216.8 | 394.1 | 1292.9 | 2744.0 | 3891.1 | 6679.9 | 17218.5 | 19.3 ($r = 0.999$) | 10 | 293 |
| $Z_{25}$ | 151.0 | 952.7 | 4021.0 | 7355.8 | 10619.9 | 14985.0 | 33989.3 | 64.8 ($r = 1.000$) | 50 | 298 |
| $Z_{26}$ | 107.8 | 775.3 | 3440.5 | 6562.5 | 8780.7 | 12951.5 | 29652.2 | 64.3 ($r = 1.000$) | 33.3 | 298 |
| $Z_{27}$ | 184.8 | 315.8 | 1534.5 | 3116.9 | 4529.0 | 6983.0 | 16108.0 | 22.3 ($r = 1.000$) | 10 | 298 |

Globally, the values fit with the equation: $Z = \frac{a'\mathrm{Q}_0}{\mathrm{Q}_0 + b'\exp\left(\frac{-c'}{T}\right)}\left\{1 - \exp\left[-\mathrm{Q}_0 d'T\exp\left(\frac{-e'}{T}\right)t\right]\right\} + f'$. This is identical to Eq. (8). Its parameters and coefficient are: $a' = 33200$, $b' = 1.194 \times 10^{-15}$, $c' = 9930$, $d' = 0.001206$, $e' = 2680$, $f' = 707$, $r = 0.993$, $s = 95.8 \times 10^6$.

Table 4
Influence of viscosity

| $t$ (min) | 0 | 15 | 60 | 150 | 240 | ∞ | $v_0$ | $M_0$ | $\eta$(mPa s) |
|---|---|---|---|---|---|---|---|---|---|
| $Z_{28}$ | 335.5 | 611.0 | 839.3 | 1355.6 | 1883.1 | 4285.7 | 10.3 ($r=0.997$) | 20 | 1.368 |
| $Z_{29}$ | 188.5 | 704.1 | 1874.0 | 3191.8 | 4108.0 | 9066.0 | 35.9 ($r=1.000$) | 40 | 1.368 |
| $Z_{30}$ | 241.6 | 1050.7 | 2268.1 | 4647.2 | 6172.2 | 14739.5 | 36.8 ($r=0.999$) | 70 | 1.368 |
| $Z_{31}$ | 543.1 | 1520.9 | 3167.5 | 6417.0 | 8568.8 | 20886.2 | 46.4 ($r=0.999$) | 100 | 1.368 |
| $Z_{32}$ | 243.7 | 537.7 | 785.8 | 1340.9 | 2173.4 | 4847.6 | 11.7 ($r=0.998$) | 20 | 1.458 |
| $Z_{33}$ | 325.5 | 779.0 | 1346.8 | 2593.4 | 3610.7 | 8628.1 | 18.7 ($r=0.999$) | 40 | 1.458 |
| $Z_{34}$ | 192.5 | 717.0 | 2232.2 | 4785.7 | 5851.5 | 17957.0 | 34.2 ($r=1.000$) | 70 | 1.458 |
| $Z_{35}$ | 236.1 | 939.5 | 2551.9 | 5440.1 | 7409.7 | 22423.3 | 40.8 ($r=1.000$) | 100 | 1.458 |
| $Z_{36}$ | 463.4 | 792.5 | 834.5 | 1395.0 | 1547.1 | 4187.3 | 5.4 ($r=0.977$) | 20 | 1.577 |
| $Z_{37}$ | 262.0 | 593.8 | 994.8 | 2045.6 | 3431.4 | 8089.5 | 13.5 ($r=0.999$) | 40 | 1.577 |
| $Z_{38}$ | 321.5 | 729.5 | 1542.2 | 3373.8 | 4689.6 | 13199.8 | 19.2 (r = 1.000) | 70 | 1.577 |
| $Z_{39}$ | 149.1 | 581.4 | 2088.5 | 4824.7 | 6249.0 | 19885.0 | 30.5 (r = 1.000) | 100 | 1.577 |
| $Z_{40}$ | 203.6 | 374.3 | 562.3 | 1045.1 | 1229.0 | 3521.3 | 5.8 (r = 0.997) | 20 | 1.745 |
| $Z_{41}$ | 458.7 | 658.2 | 1049.0 | 2022.0 | 2639.1 | 7576.5 | 8.4 (r = 1.000) | 40 | 1.745 |
| $Z_{42}$ | 439.9 | 510.8 | 1183.3 | 2501.9 | 4408.2 | 13801.4 | 12.2 (r = 1.000) | 70 | 1.745 |
| $Z_{43}$ | 309.5 | 667.5 | 1372.1 | 3616.0 | 5626.0 | 17224.1 | 12.6 (r = 1.000) | 100 | 1.745 |

Globally, the values fit with the equation: $Z=\frac{a''M_0}{(c''+\eta)}\{1-\exp[-(d''/(1+b''\eta)-e'')t]\}+f''$. This is identical to Eq. (9). Its parameters and coefficient are: $a''=462$, $c''=0.796$, $d''=0.0893$, $b''=0.0252$, $e''=0.0842$, $f''=404$, $r=0.997$, $s=11.0\times10^6$.

Which can be reduced to the previous one provided $A=0$ and $B=1$. Finding the value of $k^v$ in the previous equation, substituting it in lieu of $b$ and $d$ (which include the $k_2$ constant) in Eq. (7), and simplifying, we then have:

$$Z=\frac{a''M_0}{(c''+\eta)}\{1-\exp[-(d/(1+b''\eta)-e'')t]\}+f'' \quad (9)$$

### 3.4. Influence of ionic strength. Experiments 44–59, Table 5, Fig. 1d

If the following is done in Eq. (7):

$$aQ_0/(Q_0+c)=a''' \quad M_0+f\ll eQ_0$$

$$d=d'''\exp(z_M z_Q|^{1/2})$$

By putting the constants together and simplifying, then we have:

$$Z=\frac{a'''M_0}{(M_0+b''')}\{1-\exp[-d'''\exp(e'''I^{1/2})]\}+f''' \quad (10)$$

Parameter $e'''$ contain the product of the charges of the reagents, its value indicating that the reaction takes place between species with small charges and opposite signs.

## 4. Conclusions

Global reaction is a two-stage mechanism: in the first one IGFBP-3 reacts with antibody P and in the second one the M-labelled antibody binds to the PQ immunocomplex. The second stage is slower and so determined the rate of the global reaction.

The concentration of the labelled immunocomplex relates to $P_0$, $Q_0$, $M_0$ as per a mono-exponential rate equation corresponding to a reversible second-order process that can be attributed to a single type of binding site.

The influence of viscosity on the apparent rate constant for the formation of the immunocomplex is explained by admitting that the approximation stage rate decreases. The resulting expressions are justified by the introduction of the value of the obtained constant as per Kramers' equation in the corresponding rate equations.

Ionic strength has low influence on the rate constant. The reaction is slower as ionic strength rises. This suggests that the reacting species have small electrical charges and opposite signs. According to this, the kinetic variation resulting from the different glycerol concentrations used

Table 5
Influence of ionic strength ($Q_0 = 50$)

| $t$ (min) | 0 | 15 | 60 | 150 | 240 | ∞ | $v_0$ | $M_0$ | $I$ |
|---|---|---|---|---|---|---|---|---|---|
| $Z_{44}$ | 355.5 | 705.0 | 1171.8 | 2040.8 | 2571.9 | 4524.9 | 15.5 ($r = 0.999$) | 20 | 0.023 |
| $Z_{45}$ | 221.6 | 668.2 | 2166.1 | 3651.1 | 4525.5 | 8255.0 | 41.2 ($r = 1.000$) | 40 | 0.023 |
| $Z_{46}$ | 254.3 | 1041.9 | 3122.2 | 5815.9 | 7137.9 | 13261.0 | 56.2 ($r = 1.000$) | 70 | 0.023 |
| $Z_{47}$ | 454.0 | 1341.8 | 4343.5 | 7739.0 | 9610.7 | 17422.7 | 78.7 ($r = 1.000$) | 100 | 0.023 |
| $Z_{48}$ | 532.0 | 555.4 | 1030.2 | 1896.5 | 2816.9 | 4687.3 | 7.5 ($r = 0.999$) | 20 | 0.047 |
| $Z_{49}$ | 332.0 | 823.0 | 1828.9 | 3468.5 | 4591.2 | 7783.2 | 28.2 ($r = 1.000$) | 40 | 0.047 |
| $Z_{50}$ | 190.2 | 929.7 | 3162.2 | 5917.7 | 7385.0 | 13193.0 | 58.7 ($r = 1.000$) | 70 | 0.047 |
| $Z_{51}$ | 246.0 | 1153.0 | 3681.4 | 7113.3 | 9042.4 | 17973.5 | 66.2 ($r = 1.000$) | 100 | 0.047 |
| $Z_{52}$ | 406.1 | 629.0 | 1179.0 | 2168.0 | 2429.9 | 4297.3 | 12.5 ($r = 1.000$) | 20 | 0.070 |
| $Z_{53}$ | 267.3 | 683.6 | 1682.4 | 3181.5 | 4475.3 | 7708.3 | 27.6 ($r = 1.000$) | 40 | 0.070 |
| $Z_{54}$ | 350.5 | 983.0 | 2633.0 | 5087.1 | 6726.6 | 12449.8 | 43.2 ($r = 1.000$) | 70 | 0.070 |
| $Z_{55}$ | 185.0 | 904.0 | 3699.0 | 6960.1 | 9749.5 | 18334.5 | 71.7 ($r = 1.000$) | 100 | 0.070 |
| $Z_{56}$ | 240.5 | 415.0 | 1096.6 | 1911.8 | 2345.4 | 4296.8 | 16.7 ($r = 1.000$) | 20 | 0.094 |
| $Z_{57}$ | 431.1 | 1112.2 | 1854.5 | 3268.0 | 4062.3 | 7579.2 | 27.8 ($r = 0.997$) | 40 | 0.094 |
| $Z_{58}$ | 287.2 | 605.2 | 2405.9 | 5032.9 | 6999.1 | 13805 | 37.5 ($r = 0.999$) | 70 | 0.094 |
| $Z_{59}$ | 339.5 | 912.5 | 3462.4 | 6943.5 | 8883.2 | 17411.7 | 56.9 ($r = 1.000$) | 100 | 0.094 |

Globally, the values fit with the equation: $Z = \frac{a'''M_0}{(M_0 + b''')}\{1 - \exp[-d'''\exp(e'''I^{1/2})]\} + f'''$. This is identical to Eq. (10). Its parameters and coefficient are: $a = 115900$, $b = 570$, $d = 0.00402$, $e = -0.965$, $f = 419$, $r = 0.998$, $s = 6.54 \times 10^6$.

does not seem to be due to the influence of the dielectric constants of the solutions; hence, it can only be attributed to viscosity. The influence of temperature on equilibrium and kinetics is shown by van t'Hoff's and Eyring's equations, respectively. Activation enthalpy is estimated to be 5360 cal/mol, with the magnitude order of the viscous flow energy of water. The last three conclusions suggests diffusive control for the process.

## References


[1] L.E.M. Miles, C.N. Hales, Immunoradiometric assay procedures: new developments. In in vitro procedures with radioisotopes in medicine. Viena (1970) 483–484.

[2] C. Olivas Arroyo, J.L. Moreno Frigols, Influence of viscosity and ionic strength on the reaction kinetics of aldosterone and androstendione and their specific antibodies, Journal of Pharmaceutical and Biomedical Analysis 26 (2001) 547–562.

[3] C. Olivas Arroyo, M.J. Duart Duart, J.L. Moreno Frigols, Kinetics and equilibrium in insulin radioimmunoassay, Journal of Immunoassay and Immunochemistry, in press.

[4] M. Stenberg, L. Stiblert, External diffusion in solid-phase immunoassays, Journal of Theoretical Biology 120 (1986) 129–140.

[5] H. Nygren, M. Werthen, M. Stenberg, Kinetics of antibody binding to solid-phase-immobilised antigen. Effect of diffusion rate limitation and steric interaction, Journal of Immunological Methods 101 (1988) 63–71.

[6] H. Nygren, M. Stenberg, Immunochemistry at interfaces, Immunology 66 (1989) 321–327.

[7] M. Stenberg, H. Nygren, Kinetics of antigen–antibody reactions at solid–liquid interfaces, Journal of Immunological Methods 113 (1988) 3–15.

[8] G. Weber, The binding of small molecules to proteins, in: B. Pullman, M. Weissblut (Eds.), Molecular Biophysics, Academic Press, New York, 1965 p. 369.

[9] H.J. Motulsky, L.C. Mahan, The kinetics of competitive radioligand binding predicted by the law of mass action, Molecular Pharmacology 25 (1984) 1.

[10] M. Karlsson, A. Neil, Estimation of binding parameters by kinetic data analysis: differentiation between one and two binding sites, European Journal of Pharmacology 148 (1988) 115–125.

[11] K.A. Xavier, R.C. Willson, Association and dissociation kinetics of anti-hen egg lysozime monoclonal antibodies HyHEL-5 and HyHEL-10, Biophysical Journal 74 (1998) 2036–2045.

[12] K.A. Xavier, S.M. McDonald, J.A. McCammon, R.C. Willson, Association and dissociation kinetics of bobwhite quail lysozyme with monoclonal antibody HyHEL-5, Protein Engineering 12 (1999) 79–83.

[13] P.W. Atkins, Physical Chemistry, Oxford University Press, 1983.

[14] H.A. Kramers, Brownian motion in a field of force and the diffusion model of chemical reactions, Physica 7 (1940) 284–304.